intersection gap heating may be three times the surface heating.

In summary, the results of the experimental study show that the heating to RSI tile surfaces is significantly increased in some areas. As would be expected, the largest increase occurs on a tile which protrudes above the others. Heating on the upstream face of a tile is strongly affected by the interacting longitudinal gap flow. In flight, flow developing in 6-in. long longitudinal gaps is expected to produce heating rates several times the corresponding smooth surface heating rates where the boundary layer is thin, but have little or no effect under thick boundary-layer conditions.

References

[1] Anderson, R. W., Brooks, W. A., Jr., Leonard, R. W., and Maltz, J., "Shuttle, Structures—A Technology Overview," *Astronautics and Aeronautics*, Vol. 9, No. 2, Feb. 1971, pp. 38–47.

[2] Hello, S., "The Space Shuttle Program—Progress and Plans," AIAA/ASME/SAE 14th Structures Structural Dynamics and Materials Conference, March 20–22, 1973, Williamsburg, Va.

[3] Love, E. S., "Advanced Technology and the Space Shuttle," *Astronautics and Aeronautics*, Vol. 11, No. 2, Feb. 1973, pp. 30–66.

[4] Dunavant, J. C. and Stone, H. W., "Effects of Roughness on Heat Transfer to Hemisphere Cylinders at Mach Numbers 10.4 and 11.4," TN D-3871, March 1967, NASA.

[5] Johnson, C. B., "Heat Transfer Data to Cavities Between Simulated RSI Tiles at Mach 8," CR-128, 770, June 1973, (Space Shuttle DMS-DR-2043), NASA.

Correlation of Radiative Heating Calculations for Venus Entry

C. T. EDQUIST*

Martin Marietta Corporation, Denver, Colo.

ESTIMATES of the effect of configuration and trajectory changes on entry aeroheating are valuable for a quick assessment of possible alternative configurations and/or launch opportunities. The proper correlating parameters for convective heating are well known.[1] Since radiative heating is a significant fraction of the total for Venus entry, a complete assessment of the heat shield design requires a correlation of the radiative as well as the convective heat load.

Entry heating calculations have been performed for a number of configuration and trajectory combinations in support of a Venus entry study.[2] Table 1 lists the entry velocity V_E, entry angle γ_E, ballistic coefficient β, cone angle θ_c, and nose radius R_n for each of the cases examined. The basic shape considered was a sphere-cone but three Apollo-like configurations, essentially spherical segments, were also included. The radiative heat flux histories to the wall at the stagnation point and at a forebody point located radially at about two-thirds of the base radius were determined. Although the study was not specifically parametric, a wide enough range of the parameters of interest was included so that correlation of the results could be attempted.

Only a brief description of the calculation procedure[2] will be given here. Basically, an uncoupled analysis was made. That is, convective, radiative, and ablative phenomena were considered separately and then correction factors were applied where appropriate. In this situation, calculation of the radiative flux requires a solution for the inviscid flowfield to provide the necessary shock layer thickness and thermodynamic variables.

Received November 30, 1973; revision received January 31, 1974.
Index category: Radiation and Radiative Heat Transfer.

* Staff Engineer. Member AIAA.

Table 1 Venus trajectory and geometry parameters and radiative heating results

Case	V_E km/s	γ_E deg	β kg/m^2	θ_c deg	R_n m	q_{c_m}' MW/m^2	Q_c' MJ/m^2	q_{r_m}' MW/m^2	Q_r' MJ/m^2
1	11.16	40	78.54	60	0.1586	4.51	9.71	5.85	10.2
2		40	78.54	60	0.3683	7.05	15.0	9.00	16.0
3		40	78.54	60	0.5525	8.58	17.6	10.5	19.5
4		40	78.54	55	0.5080	8.35	17.7	7.80	14.6
5		40	78.54	70	0.3683	8.00	16.9	13.2	26.0
6		40	78.54	AP	1.585	15.7	31.0	13.7	25.1
7		40	78.54	AP	2.378	18.6	36.4	16.7	31.9
8		20	125.7	45	0.1346	3.33	13.8	1.84	4.80
9		40	125.7	45	0.1346	7.80	16.4	3.90	5.89
10		55	125.7	45	0.1346	9.40	16.1	4.90	6.58
11		20	125.7	AP	0.5734	6.55	27.9	6.20	24.6
12	11.34	35	86.40	60	0.3975	11.3	21.6	10.8	21.7
13		40.5	90.72	60	0.3975	13.5	24.0	14.0	24.3
14		40.5	90.72	55	0.5080	14.9	26.5	11.1	20.0
15		45	119.6	55	0.2355	15.7	25.4	11.4	19.2
16		45	119.6	55	0.2753	17.3	28.0	12.0	21.2
17		15	141.4	45	0.2753	5.00	28.1	2.10	10.5
18		25	141.4	45	0.2753	11.2	32.1	4.50	12.2
19		45	141.4	45	0.2753	22.0	35.2	8.40	13.6
20		60	141.4	45	0.2753	27.1	36.6	10.3	13.6
21	11.40	35	86.40	60	0.3975	11.9	23.4	12.0	23.0
22		25	141.4	45	0.2753	12.3	34.2	4.64	13.0
23		41	141.4	45	0.2753	21.8	37.1	7.90	14.1

For the probe shapes for which the body sonic point occurs at the aft corner ($\theta_c > 50°$), a single-strip method of integral relations program for arbitrary equilibrium gas mixtures[3] was used. When the sonic point occurs on the spherical section and the cone surface is supersonic, an inverse blunt body solution coupled with the method of characteristics was used.[4] The latter calculation was made for pure CO_2 in equilibrium. All the other calculations correspond to the Venus model atmosphere presented in Ref. 5 for which the chemical composition is 97% CO_2 and 3% N_2 by volume.

With the inviscid conditions defined, a boundary-layer solution was performed including the important effect of entropy layer swallowing.[6] The radiative heat flux to the wall from an isothermal slab was calculated using the method of Nicolet.[7] The temperature and pressure of the slab were taken to be the boundary layer edge values at the body point of interest, including entropy layer swallowing, and its thickness was assumed equal to the adiabatic shock standoff distance from the inviscid analysis. Use of the boundary-layer edge temperature rather than the post shock value makes little difference in radiative heating results in the stagnation region or in the cone region for large angle cones. As the cone angle decreases, however, the temperature difference across the shock layer becomes increasingly large in contrast to the pressure difference. As a result, use of the boundary-layer edge temperature in the isothermal slab analysis leads to a somewhat conservative predicted radiative flux, while use of the post shock temperature significantly underpredicts the cone radiative heating for small cone angles. The radiative flux computed by the isothermal slab model was modified by the cooling factor shown in Fig. 1 to

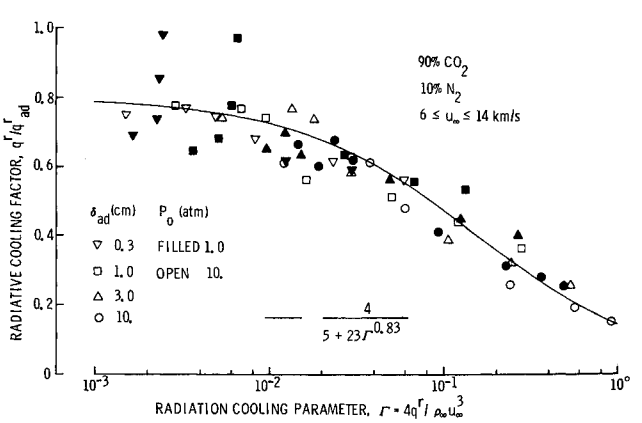

Fig. 1 Radiative cooling factor for Venus entry.

account for nonadiabatic effects. This cooling factor was developed from the theoretical work of Page and Woodward[8] for the stagnation point during Venus entry. The same technique was used at all body points, with the radiation cooling parameter modified by dividing by $\sin^3\theta_w$ to account for the smaller radiation potential as the shock strength lessens. This leads to a relatively greater cooling effect aft on the body. No correction was made for the effect of ablation products, but a Venus study[9] has shown the correction to be small for the entry velocities of present interest. The cone locations considered in the present study are at points sufficiently far forward so that the pressure is nearly Newtonian and has not begun the drop toward sonic pressure. A comparison of the present procedure with a more complete technique that includes radiative-convective coupling is contained in Ref. 2. The results show good agreement in the stagnation region (10%), with increasing differences aft on the body due, in part, to the conservative approach adopted in the present method.

Radiative heating histories for a typical trajectory and shape are depicted in Fig. 2. For this low-angle cone, the stagnation region radiative heating is significantly greater than at the cone location. For higher cone angles, however, the results may be comparable. Two distinct relative maxima are noted in the pulses, either of which may be larger depending on the trajectory. Early in the trajectory, before significant deceleration has occurred, the shock layer experiences low pressures and high temperatures that lead to high dissociation and ionization levels. Therefore, a large fraction of the radiation results from atomic line and continuum processes. As the probe decelerates, the pressure continues to rise but the temperature drops, leading to an increase in the molecular population and resulting radiation from molecular band systems. For the present trajectories, this transition in radiative processes occurs near the time of peak stagnation point convective heating. The lower shock-layer temperatures away from the stagnation point may shift the time and magnitude of this change, but the same phenomenon also occurs at cone locations. In general, for the cases shown in Table 1, the first radiation peak was the greater of the two at the stagnation point, while the reverse was true at the cone locations considered.

The radiative heating values of most interest are the maximum heating rate sustained at the stagnation point $q_{o_m}{}^r$ and at the off-stagnation point location $q_{c_m}{}^r$ and the integrated heating at the same locations, $Q_o{}^r$ and $Q_c{}^r$, respectively. Table 1 presents these results for each case as calculated by the procedure just discussed. The grouping of parameters chosen for the correlation is

$$q^r = CR_n{}^a(\beta \sin\gamma_E)^b(\sin\theta_c)^c V_E{}^d$$

$$Q^r(V_E \sin\gamma_E) = KR_n{}^a(\beta \sin\gamma_E)^b(\sin\theta_c)^c V_E{}^d$$

The dependence of radiation on velocity is extremely strong. The initial correlation attempts were made within the groups of constant velocity and the velocity term was combined with the constant. No elaborate curve-fitting procedure was used, but rather a best visual fit with some allowance made to keep

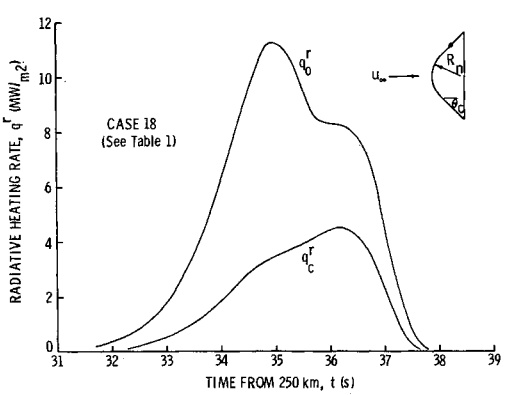

Fig. 2 Radiative heating rate histories for Venus entry.

Table 2 Venus radiative heating correlation constants

V_E	$C_o V_E{}^d$	$K_o V_E{}^{d-1}$	$C_c V_E{}^d$	$K_c V_E{}^{d-1}$
11.16	0.085	0.116	0.218	0.236
11.34	0.130	0.149	0.250	0.294
11.40	0.143	0.163	0.278	0.320

the exponents relatively simple was applied. The exponents a, b, and c were found to be $a = 0.50$, $b = 1.25$, $c = 4.75$. Combining the velocity variation and constants resulted in Table 2.

The success of the correlations is demonstrated in Fig. 3 where the results from the correlation are plotted against the values from the calculation for both the stagnation point and cone location. Both heating rate and total heating are shown with the filled symbols denoting the total heating comparison. With few exceptions, the correlation represents the calculation within 10%. As noted in Table 1, the correlations cover a factor of nearly 18 in nose radius, over 3 in $\beta \sin\gamma_E$, entry angles from 15° to 60°, and cone angles from 45° to 70°. Examination of Fig. 3 shows that the three symbols falling below the ±10% band correspond to Case 5 for which the cone angle is 70°. For this large angle, the shock layer in the stagnation region is influenced by the subsonic flow on the cone to the extent that the stagnation point velocity gradient is reduced and the shock standoff distance is increased over that expected for a sphere at the same freestream conditions. The resulting reduction in stagnation point convective heating usually is accounted for by determining an effective nose radius R_{eff} larger than the actual R_n. If this larger radius is used also in the correlation equation for radiative heating, values within the 10% error band are obtained. The point in Fig. 3 above the 10% error band corresponds to the maximum stagnation point radiative heating rate for Case 17. The entry angle for this case is 15°, the lowest considered. The correlation equation shows the heating rate to be more sensitive to the entry angle than is the total heating. Of course, the flight-path angle does not remain constant during a ballistic trajectory but decreases to a minimum value before finally increasing. At low initial flight-path angles, the percentage decrease is a more significant fraction of the entry value. This smaller effective entry angle could account for the discrepancy between correlation and calculation at this low γ_E.

Figure 3 shows that the cone values of heating rate and total heating could be correlated as successfully as their counterparts at the stagnation point. The Apollo shapes were omitted from the off-stagnation point body-angle correlation. It should be noted that for the entry velocity range considered, single values of a, b, and c correlated the results equally well for each velocity group and both body locations.

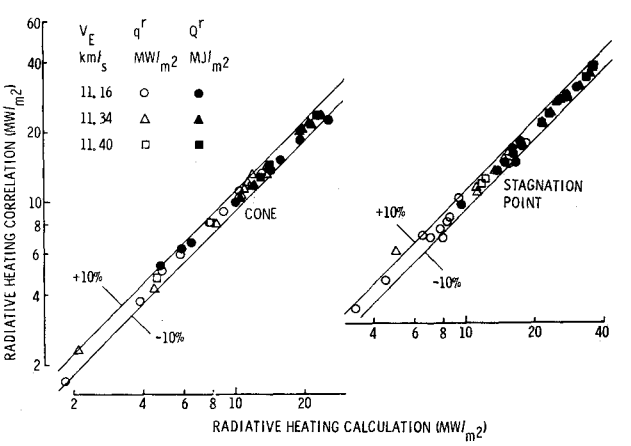

Fig. 3 A comparison of analytical and correlated radiative heating for Venus entry.

Although the velocity range considered was small, significant changes in the radiation were observed as velocity was varied. Correlations of the results were attempted in the manner suggested by the equations given previously. It was determined that the results could be well represented in that form. However, in contrast to the correlation with the other parameters in which single values of a, b, and c represented each velocity and location and both the heating rate and total heating, separate values of d for each location and both heating rate and total, heating were necessary to correlate the velocity-dependent calculations. These four values and the resulting constants are

$$C_o = 6.17 \times 10^{-26} \qquad K_o = 1.09 \times 10^{-18}$$
$$d = 23.1 \qquad d = 17.2$$
$$C_c = 3.04 \times 10^{-15} \qquad K_c = 1.06 \times 10^{-16}$$
$$d = 13.2 \qquad d = 15.6$$

This necessity for different values of d is not surprising considering the diverse radiative processes occurring during entry in a CO_2–N_2 atmosphere. As seen in Fig. 2 and described earlier, two basic regimes are encountered. As the entry velocity is increased, a larger contribution from the line and continuum processes is encountered. At the lower temperatures away from the stagnation point, the radiation from the molecular band systems remains of major importance to higher entry velocities. As might be expected, the exponents for the total heating for both body locations are nearly equal since the integration tends to average the contributions from the various radiative processes over each trajectory. Because of the extreme sensitivity to entry velocity, care should be taken in using the exponents d outside the velocity range from which they were derived.

The radiative heating results from a series of Venus entry heating calculations have been correlated in terms of the usual trajectory and geometry parameters. The radiation calculation technique employed is an uncoupled one which allows economical consideration of a large number of cases, while still providing reasonable agreement with results of a more elaborate procedure. Within the admittedly small entry velocity range considered, the maximum heating rate and total heating at the stagnation point and at an off-stagnation location were correlated successfully. Single exponents for all velocities represented the variations of nose radius, cone angle, ballistic coefficient, and entry angle. Separate velocity exponents were required for each location and for both heating rate and total heating. With few exceptions, the calculated values could be predicted within 10%. Perhaps the best use of these correlations would be to extrapolate to other shapes, ballistic coefficients, and entry angles from detailed trajectory calculations for one combination of these values at a given entry velocity.

References

[1] Allen, H. J. and Eggers, J. A., Jr., "A Study of the Motion and Aerodynamic Heating of Missiles Entering the Earth's Atmosphere at High Supersonic Speeds," TN 4047, Oct. 1957, NACA.

[2] "System Design Study of the Pioneer Venus Spacecraft—Final Report," CR 114592, TRW Rept. 2291-6005-RU-00, July 29, 1973, NASA.

[3] Edquist, C. T., "The Method of Integral Relations for Spherically Blunted Bodies with Sharp Sonic Corners in an Equilibrium Gas Mixture," MMC R72-48671-001, July 1972, Martin Marietta Corp., Denver, Colo.

[4] Inouye, M., Rakich, J. V., and Lomax, H., "A Description of Numerical Methods and Computer Programs for Two-Dimensional and Axisymmetric Supersonic Flow Over Blunt-Nosed and Flared Bodies," TN D-2970, Aug. 1965, NASA.

[5] "Models of the Venus Atmosphere," SP 8011, Sept. 1972, NASA.

[6] Edquist, C. T., "A Technique for Predicting Shock Induced Vorticity Effects During Venus Entry," MMC R70-48671-006, Aug. 1970, Martin Marietta Corp., Denver, Colo.

[7] Nicolet, W. E., "User's Manual for the Generalized Radiation Transfer Code (RAD/EQUIL)," Rept. UM-69-9, Oct. 1969, Aerotherm Corp., Mountain View, Calif.

[8] Page, W. A. and Woodward, H. T., "Radiative and Convective Heating During Venus Entry," *AIAA Journal*, Vol. 10, No. 10, Oct. 1972, pp. 1379–1381.

[9] Sutton, K., "Fully Coupled Nongray Radiating Gas Flows with Ablation Products Effects About Planetary Entry Bodies," *AIAA Journal*, to be published.

Shuttle Extra-Vehicular Life Support Equipment

JAMES G. SUTTON*

Hamilton Standard United Aircraft Corporation, Windsor Locks, Conn.

I. Introduction

THE primary objective of the Space Shuttle Program is to provide a new space transportation capability that will substantially reduce the cost of space operations and provide

Mission Duration	4 Hours
Metabolic loads	
• Average	1000 Btu/hr
• Minimum	400 Btu/hr
• Peak	1600 Btu/hr
O_2 Supply	1.04 lbs
Pressure Control	8.2 ± 0.2 psi
CO_2 Control	7.6 mm Hg maximum
Contaminant Control	
• Particulate	Debris trap/filter
Thermal Control	
• Heat Loads	1921 Btu/hr average 2559 Btu/hr peak
• Mode of Cooling	Liquid Cooling
• Temperature Control	Manual
Humidity Control	50°F dew point maximum
Ventilation	6 ACFM minimum
Power	220 watt-hours minimum
Communications	
• Primary	Duplex
• Backup	Simplex
Telemetry	As req'd for checkout prior to EVA and status monitoring during EVA
Life	
• Shelf	15 years
• Operational	6000 hours

Fig. 1 PLSS requirements.

Presented as Paper 73-1333 at the AIAA Crew Equipment Systems Conference, Las Vegas, Nev., November 7–9, 1973; submitted November 21, 1973; revision received January 30, 1974.

Index categories: Extra-Vehicular Activity; Spacecraft Habitability and Life Support Systems.

* Senior Engineer, Advanced Systems. Associate Fellow AIAA.